

Article

Onsite Testing for Nonlinear Analysis of an Earthquake Damaged Historical Church in Italy

Silvia Santini, Carlo Baggio, Valerio Sabbatini * and Claudio Sebastiani

Department of Architecture, Roma Tre University, L.go G.B. Marzi 10, 00153 Rome, Italy; silvia.santini@uniroma3.it (S.S.); carlo.baggio@uniroma3.it (C.B.); claudio.sebastiani@uniroma3.it (C.S.)

* Correspondence: valerio.sabbatini@uniroma3.it

Abstract: Analysis and diagnosis of historical masonry buildings are frequently affected by uncertainties due to unexpected behaviors caused by cumulative damage, material decay or transformations. This research work follows a methodology in the structural analysis of the historical masonry church of San Filippo Neri in Macerata, severely damaged after the Central Italy Earthquake occurred in October 2016. The PRiSMa laboratory (Proof testing and Research in Structures and Materials) of Roma Tre University carried out an extensive onsite testing campaign, including NDT tests as sonic tomography and endoscopy, and minor destructive technique as double flat jack test, together with dynamic monitoring under ambient vibrations, to investigate the state of conservation of the building. The onsite testing results were then implemented in an accurate finite element model, which was tuned up by means of global dynamic response provided by OMA (operational modal analysis) and updated, after the sensitivity analysis, through the Douglas-Reid method. Finally, nonlinear static and dynamic analyses were performed to investigate the state of damage of the church and reduce its uncertainties. This methodology will support the design of strengthening measures to achieve a higher level of safety concerning both needs of protection and conservation, thereby avoiding ineffectual or amiss interventions.

Keywords: historical church; onsite testing; NDT; OMA; model updating; nonlinear analysis

Citation: Santini, S.; Baggio, C.; Sabbatini, V.; Sebastiani, C. Onsite Testing for Nonlinear Analysis of an Earthquake Damaged Historical Church in Italy. *Appl. Sci.* **2021**, *11*, 11755. <https://doi.org/10.3390/app112411755>

Academic Editor: Fabrizio Balsamo

Received: 10 November 2021

Accepted: 8 December 2021

Published: 10 December 2021

Publisher's Note: MDPI stays neutral with regard to jurisdictional claims in published maps and institutional affiliations.



Copyright: © 2021 by the authors. Licensee MDPI, Basel, Switzerland. This article is an open access article distributed under the terms and conditions of the Creative Commons Attribution (CC BY) license (<https://creativecommons.org/licenses/by/4.0/>).

1. Introduction

Safety assessment and conservation work have been central activities for the construction management of historical buildings. These two activities, obviously related to each other, connect the history of a building to its future. For seismic countries with meaningful architectural heritage, the seismic safety assessment embodies a permanent work that evolves in time based on the information collected from past seismic events.

In this scenario, historical masonry religious buildings represent delicate and valuable constructions, first for their artistic testimony but also as a symbol of a local community and the embodiment of its traditions. Religious buildings such as the Italian Baroque churches, although deeply codified, exemplify the personal impulse of the architects of that period to experiment shapes and forms, which sometimes lead to premature damage (i.e., the collapse of the bell towers of Saint Peter in Rome designed by Bernini [1]).

The prediction of the structural behavior of historical masonry buildings is a complex task to accomplish where the expected response is often misleading from the real one [2]. Different strategies have been developed to approach masonry structural analysis: limit analysis, simplified methods, FEM macro- or micro-modeling and discrete element methods (DEM) are considered with regard to their realism, computer efficiency, data availability and real applicability to large structures [3]. In Mendes and Lourenço [4], a numerical study for the seismic assessment of a Portuguese masonry building typology was performed using a reduced scaled model and a finite element model. The numerical model

was calibrated through the Douglas-Reid method based on the experimental natural frequencies obtained in the modal identification of a reduced scale model. After the calibration of the numerical model, nonlinear time history analysis and nonlinear static pushover analysis were carried out to simulate the performance and the crack pattern of the physical model. The capacity curves were compared; however, in this typology of building it was found that pushover analysis does not correctly simulate the failure mode of the structure. Pushover analysis proportional to the first mode shape performed better in terms of load-displacement diagram correctly simulating the in-plane behavior. In D'Ambrisi [5], the finite element model of an historical masonry tower was tuned up based on the ambient vibration test; the best fitting between the analytical and the experimental values was achieved by taking into account the effect of the adjacent construction (changing the boundary conditions) and considering different types of masonry material in the numerical model. Then, nonlinear static and dynamic analyses were performed for the seismic assessment; the comparison of the two analysis provided levels of displacement capacity for the nonlinear dynamic analysis lower than the nonlinear static, this gap evidenced the incapacity to capture the inertial effects associated with the dynamic input in the nonlinear static analysis. In Valente and Milani [6], the behavior of eight historical masonry towers have been analyzed with detailed three dimensional FE models, non-linear dynamic analyses were performed using real accelerograms and a damage plasticity material model; the results are then compared with a non-linear static procedure based on pushover analyses. It was found that the results obtained with the non-linear static procedure were in a good agreement with those obtained from the nonlinear dynamic analysis.

This work, starting from comprehensive on-site measurements on the mechanical characterization of masonry and the dynamic identification of the church of San Filippo Neri in Macerata, implements and tunes up an accurate finite element model of the construction including the ovoidal double-shell dome and elastic spring supports. The global three-dimensional model is analyzed in the nonlinear field considering static and dynamic seismic analysis, the results of the analysis are compared and discussed.

2. Preliminary Structural Assessment of San Filippo Neri in Macerata

Macerata is a small city located in central Italy. Over the years, it has maintained its historical center with the original city walls and the characteristic masonry buildings erected between the 16th and 19th century [7].

The church of San Filippo Neri dates to 1697, the building is positioned on a slope between Corso della Repubblica and Via Santa Maria della Porta as shown in Figure 1.



Figure 1. San Filippo Neri in Macerata: on its left (North side) Corso della Repubblica and on its right Via Santa Maria della Porta (South side).

In 1903, the cracking of the dome was ascertained. In 1929, two deep cracks extended over the longitudinal direction of the dome (Figure 2). After recurrent damage on the dome, some conservation works were executed in 2012, including the repair of vertical and sub-vertical cracks with traditional procedures [8]. In 2016, a series of seismic events occurred in Macerata, the major earthquake hit the city on the 24th of August with hypocentral depth at 8.1 km in Accumoli on the Monti della Laga (about 70 km from the church of San Filippo Neri). This seism had a moment magnitude (M_w) of 6.18 ± 0.07 and epicentral macroseismic intensity (I_0) of 10 [9] [10]. The series of events damaged the main structure (Figure 2 and Figure 3) and caused the closure of the church as reported in the technical documents produced by Studio Da Gai for the Diocesi of Macerata [11].

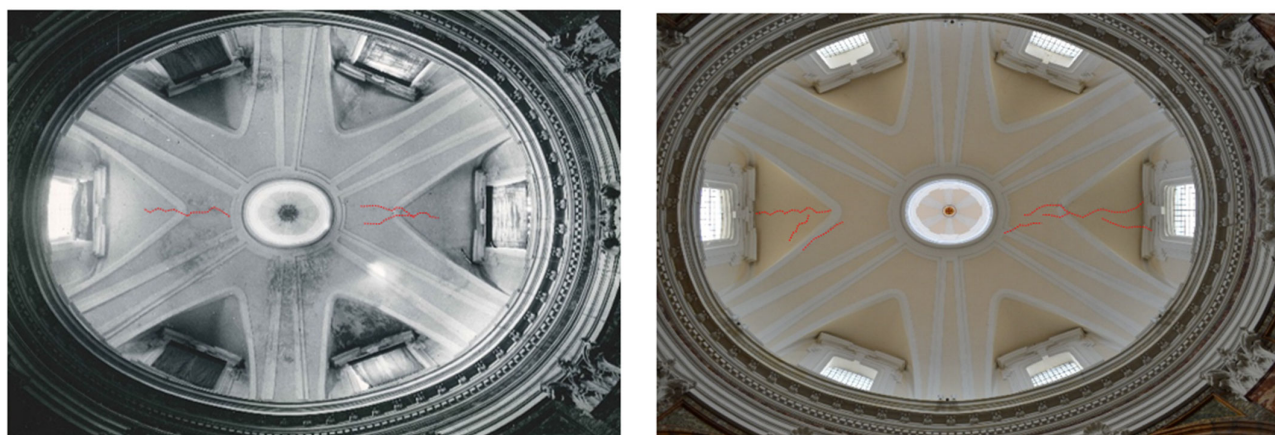


Figure 2. Recurrent longitudinal crack on the dome: on the left the conditions in 1950s, on the right the condition in 2018.



Figure 3. Details of the 2016 earthquake damage: on the right crack above the apse arch, on the left the crack in proximity of the drum.

3. Onsite Testing and Dynamic Monitoring

The laboratory of Testing and Research on Structures and Materials (PRiSMa) of the Architecture Department of Roma Tre University received from the Diocesi of Macerata the request to carry out an extensive onsite testing campaign on the church of San Filippo Neri to investigate the structural elements, characterize the mechanical properties of masonry and identify the dynamic behavior of the construction.

A total of four double flat jack tests were performed to evaluate the Young's modulus and estimate the compressive strength of masonry. Two tests (M1 and M2) were located at the street level on the exterior walls of the north and south side, one at the ground floor level on the interior masonry in proximity of the southeast pillar (M3) and one at the

basement (M4) on one of the main transversal walls of the adjacent Palazzo della Provincia as shown in Figure 4.

The locations were selected to characterize the structural elements (the pillars) and reduce the invasiveness of the tests (only M3 was performed in the interior but in a concealed area while M4 was performed in the basement, in an area inaccessible to the visitors).

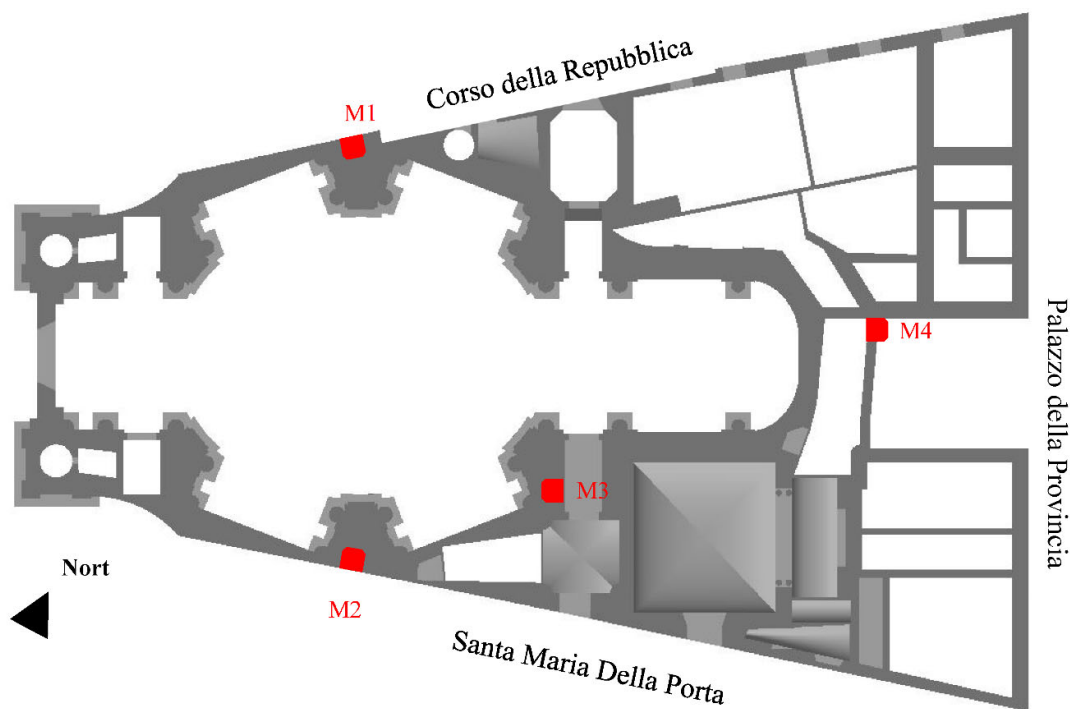


Figure 4. Double flat jack test locations.

The material under testing consists of a masonry prism with an approximated semi-circular section, the prism has a height of 500 mm and width of 350 mm as shown in Figure 5. The instrumentation includes two semicircular metal flat jacks and four Penny+Giles SLS130 linear displacement transducers positioned in the points A, B, C and D as illustrated in Figure 6. The transducers and the pressure sensor were connected to a NI SCXI 1313/1520 module and then digitally converted with a NI SCXI-1600 module, parts of NI SCXI 1001 acquisition system. The recording and visualization of the data is realized with a laptop with dedicated LabView software application. The tests followed several loading cycles to optimally evaluate the bearing capacity of masonry.

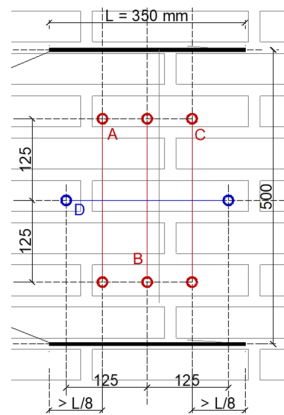


Figure 5. Double flat jack test geometry [mm].



Figure 6. Set-up of the double flat jack test.

The stress state with the modulus of elasticity was evaluated according to ASTM 1197 standard [12] and the compressive strength according to UNI 1052-1 [13], the results of the tests are reported in Table 1. The Poisson's ratio of test M4 was not evaluated due to a malfunctioning of the horizontal displacement transducers. The flat jack tests reported a significant difference in the modulus of elasticity of the masonry: southern masonry was identified as the stiffer material followed by the northern masonry and eastern masonry; the result was confirmed by unreported consolidation intervention of the exteriors orally communicated by the locals.

Table 1. Double flat jack test results.

Test	Young Modulus [MPa]	Poisson's Ratio [-]	Compressive Strength [MPa]
M1	2800	0.21	3.30
M2	4600	0.30	3.00
M3	1800	0.26	2.80
M4	1600	-	2.80

Several sonic tests were performed on the southeast pillar of the main hall with the acquisition system Boviari CMS HLF-P series SG02_0128 equipped with piezoelectric hammer. The propagation period of the sonic impulse through the masonry was measured on a mesh of 35 points (12 receivers and 23 transmitters) distanced by 25–30 cm along the two opposite sides of the pillar at a height of 158 cm from the floor level; 258 pressure wave

trajectories were processed with the dedicated algorithm of the software aTom [14], which returned the sonic tomography shown in Figure 7.

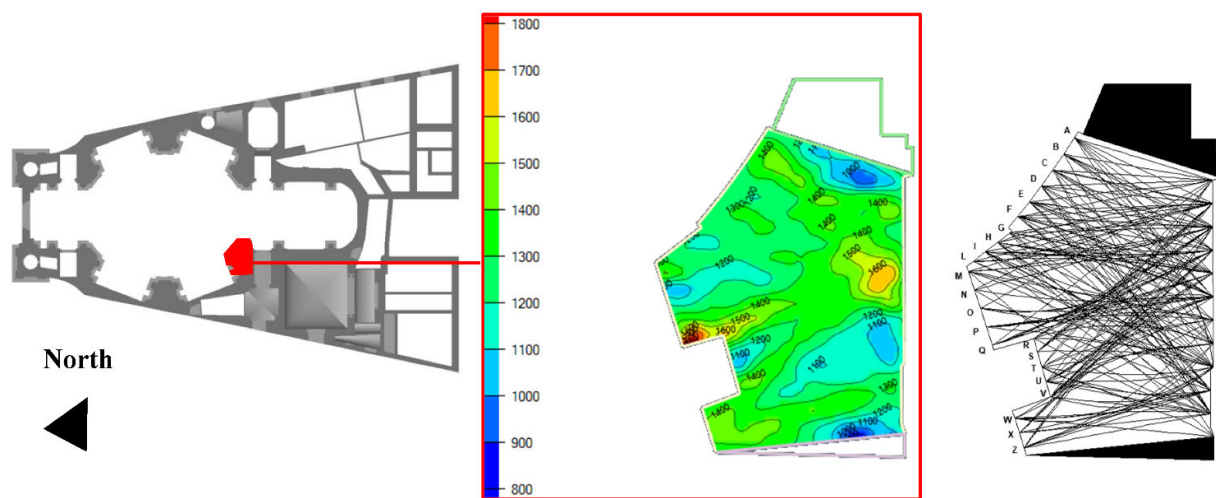


Figure 7. Sonic tomography.

The video borescope was carried out on of the same portion of masonry encompassing the sonic tomography with the RITEC RI1320 LSC video endoscopy. The qualitative inspection returned qualitatively a compact homogeneous brick masonry and few inclusions of fragmented bricks bonded well with lime mortar (Figure 8).

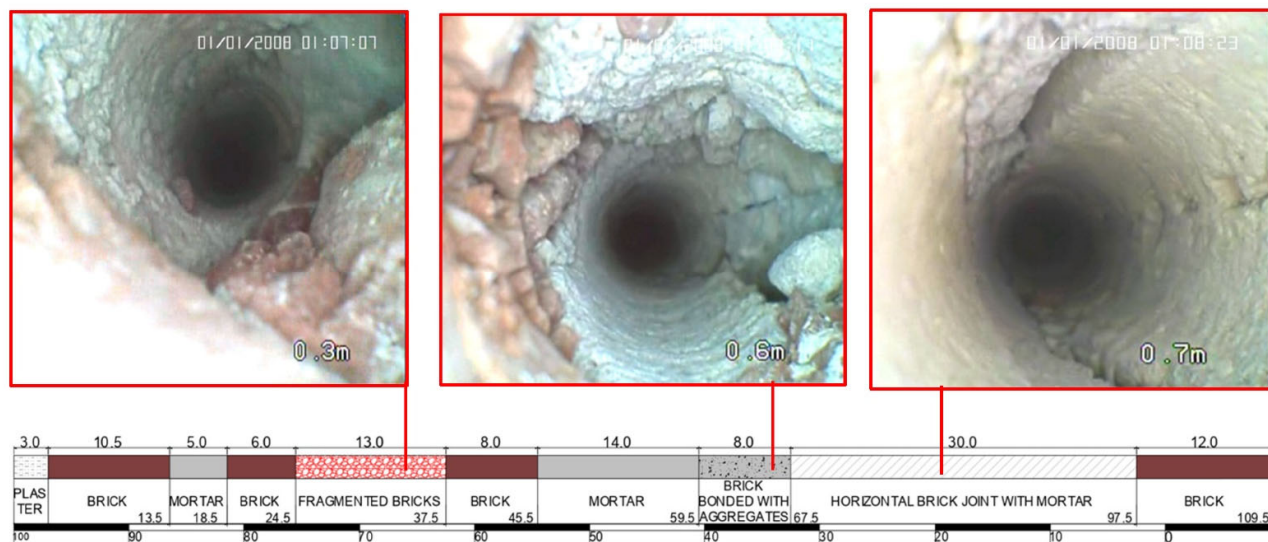


Figure 8. Video borescope inspection and derived reconstructed stratigraphy.

Considering the results from the video borescope inspection, the material was assumed to be homogeneous and isotropic material and the well-known Equation (1) was applied. Equation (1) relates the velocity of the sonic impulse (V) to the dynamic modulus of elasticity (E_d) by considering an approximated average density of the masonry (ρ) equal to 1800 kg/m³ according to the Italian Code [15] and a Poisson's ratio (ν) of 0.26 according to double flat jack test M3 executed in the same location.

$$E_d = V^2 \rho \frac{(1+\nu)(1-2\nu)}{(1-\nu)} \quad (1)$$

The sonic tomography returned a homogeneous section with an average velocity of 1250 m/s, which respectively yields to Young's moduli of 1674 MPa according to Mehta et al. [16] and 1945 MPa according to Lydon et al. [17]. It can be observed that the average value of these two estimations is the approximate value of test M3 (Table 1), thus the reliability of the double flat jack test on this type of masonry was confirmed.

The modal parameters of the church were assessed with the ambient vibration test (AVT) [18], the response acceleration of the construction was recorded for about one hour by 16 ICP piezoelectric accelerometers (PCB 393 B12, 10 V/g sensitivity, ± 0.5 g range and 8 μ g rms resolution) placed in seven points at two different levels: points A, B, C and D are located on the internal cornice of the drum at 16 m height and F, G, and C at 27.5 m height on the extrados of the dome in proximity of the lantern as shown in Figure 9.

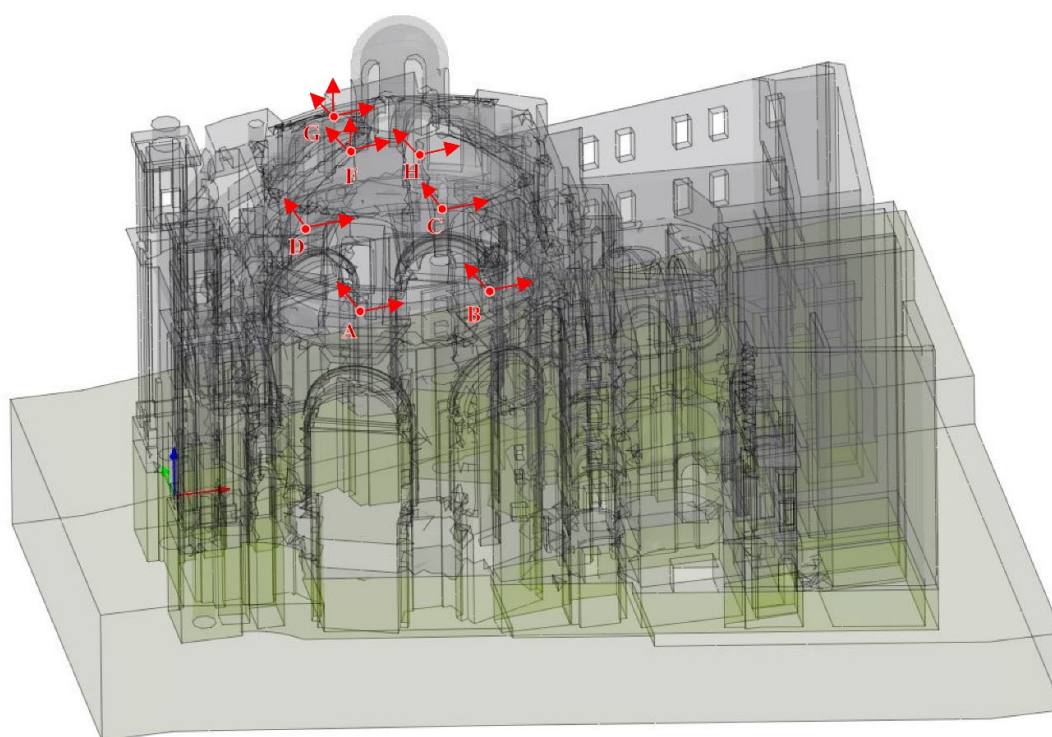


Figure 9. Ambient vibration test setup.

The data were processed according to the operational modal analysis (OMA), based on the assumption of white noise random vibrations. In this condition, it is sufficient to analyze the response of the structure (output-only modal identification) to extract the modal parameters of the building (natural frequencies, modal shape vectors and modal damping).

The signals were recorded with a sample frequency of 200 Hz and later filtered with eighth order high-pass filter at 0.7 Hz to increase the signal-to-noise ratio. The cross-power spectra were computed with 0.049 Hz frequency resolution and 5% windowing and related to the reference measurements of node B and C. The polyreference least-squares complex frequency-domain method (PolyMAX [19,20]) was applied to determine the stable poles of the approximating polynomial in correspondence of the modal parameters of the construction reported in Figure 10.

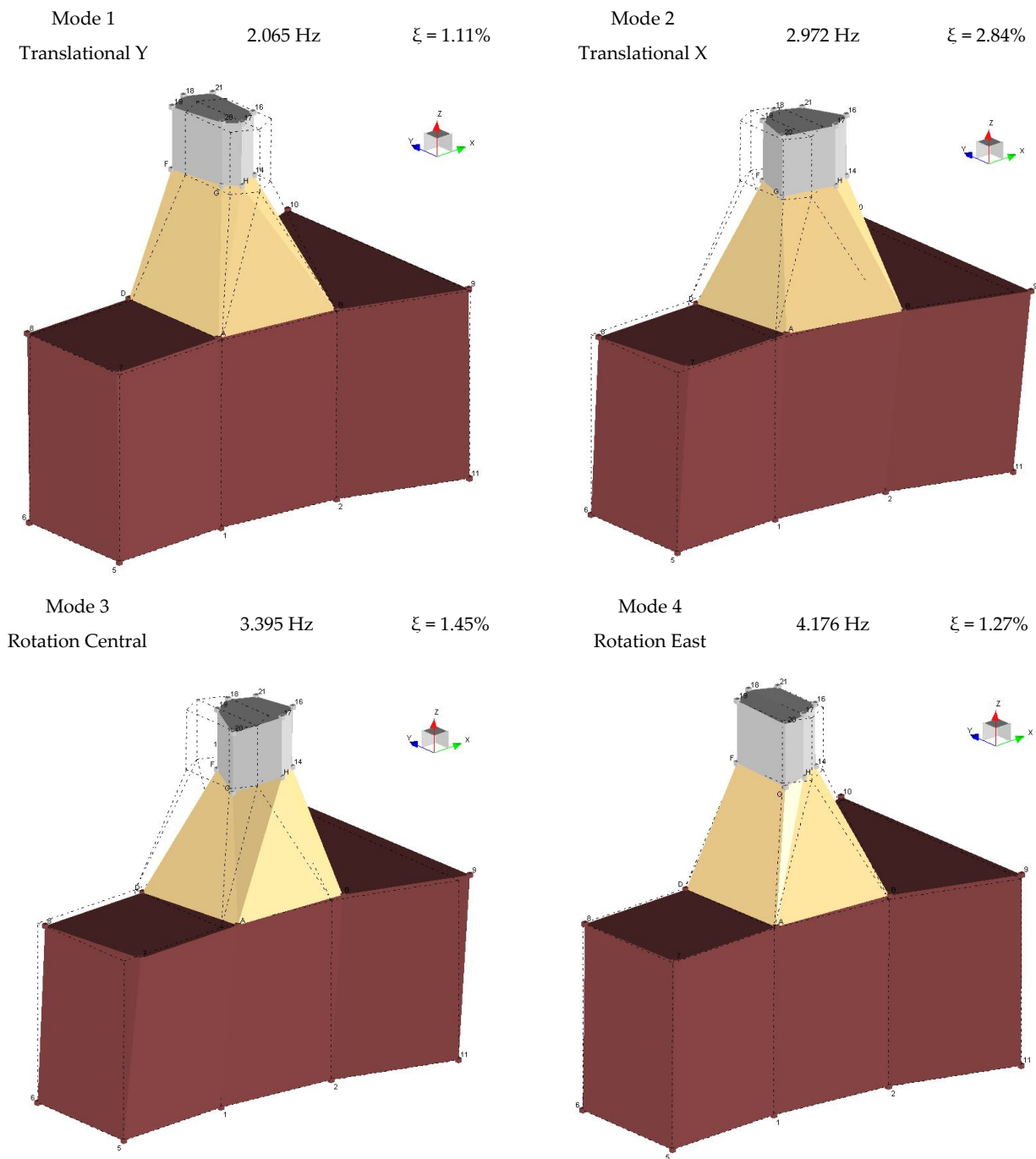


Figure 10. Results of the operational modal analysis.

The experimental modal assurance criterion (MAC) [21] shows a slight interaction between the second and third mode (24%) and a relevant dependency between the first and fourth mode (41%), as expected the rotational modes (third and fourth modes) present partial common displacements with two main translational modes (first and second modes) as shown in Figure 11.

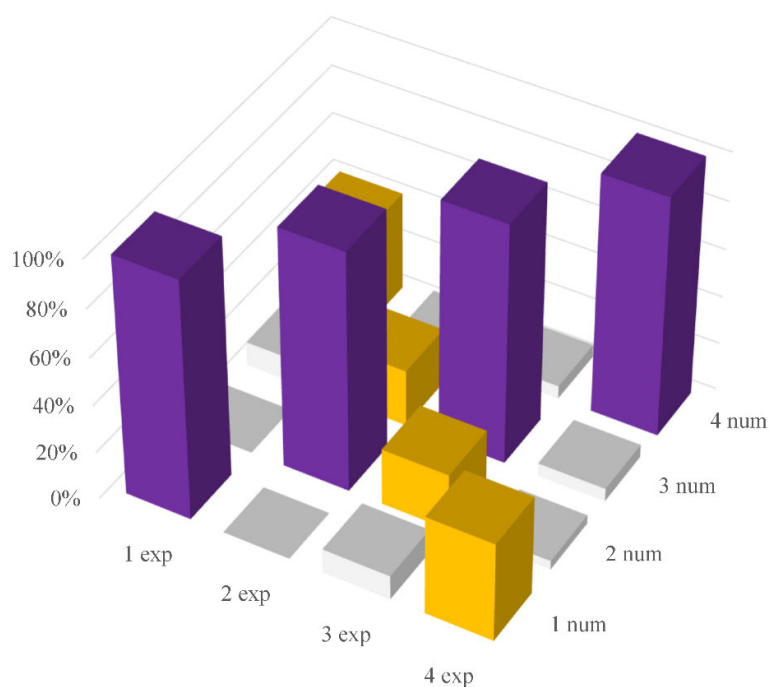


Figure 11. Modal assurance criterion between the experimental modal shapes, in yellow the detected dependencies between the modes.

4. Finite Element Model

The structural behavior of the church was studied with a tridimensional finite element model of the construction developed with the software Midas Fea NX [22]. The model is based on a three-dimensional geometrical model provided by Studio Da Gai. The foundations have been included in the model considering past geotechnical investigations. The model was processed to create a mesh of 302,138 solid tetrahedron elements. The horizontal structures, such as the wooden roofs and the reinforced concrete slabs, were modeled as lumped masses with rigid diaphragms while the more deformable and critical groin and barrel vaults in the sacristy and presbytery were accurately modeled considering constant thicknesses. The model was subdivided in nine element groups based on the architectural features, the material characteristics, the historical phases, and the identified damage (Figure 12). The soil–structure interaction was modeled with 2177 elastic three-dimensional point spring elements positioned at the base of the foundation and 11,658 elastic 2D point spring elements positioned on the lateral surfaces of the foundation walls considering as initial value a stiffness ratio of 1 to 10 between the horizontal and vertical directions (as considered by Elyamani for a similar church [23]).

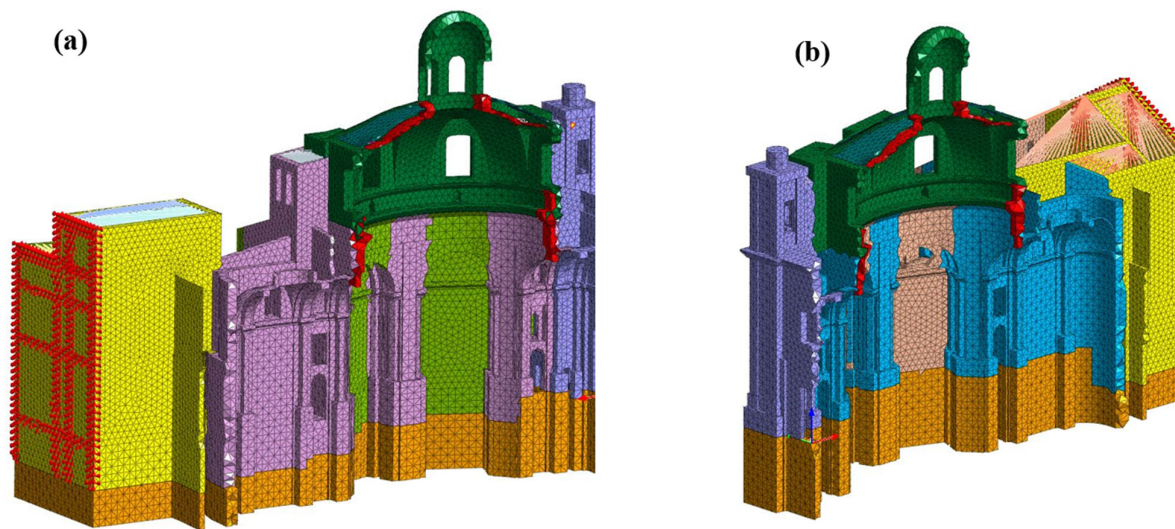


Figure 12. Section cut of the finite element model: (a) south side, (b) north side.

Particular attention was paid to the ovoidal dome. The Italian Baroque architecture of the dome origins from the models of the ancient Rome are described by Serlio [24]; during the XVII century, the dome evolved towards complex geometries with elliptical and ovoidal plans, a drum at the base and a lantern on top [25]. The dome was typically composed of two shells interconnected by ribs and surrounded by buttresses [26]. The geometrical survey reported a dome with varying thickness from 250 to 80 cm; therefore, a double shell dome with six radial ribs (in correspondence with the stuccos shown in Figure 2) was assumed and the internal cavity filled with light backing materials to transmit the lateral thrust of the intrados layer to the six buttresses was assumed. The passive resistance of the backing material (in the lower part of the cavity) was modeled with compression-only elastic springs, which link the intrados layer to the spandrels. The longitudinal crack was modeled by assigning a weaker and softer material to the region interested by damage (the damaged masonry was assumed with one fifth of the mechanical parameters of the dome). Figure 13 shows a section cut of the model of the dome.

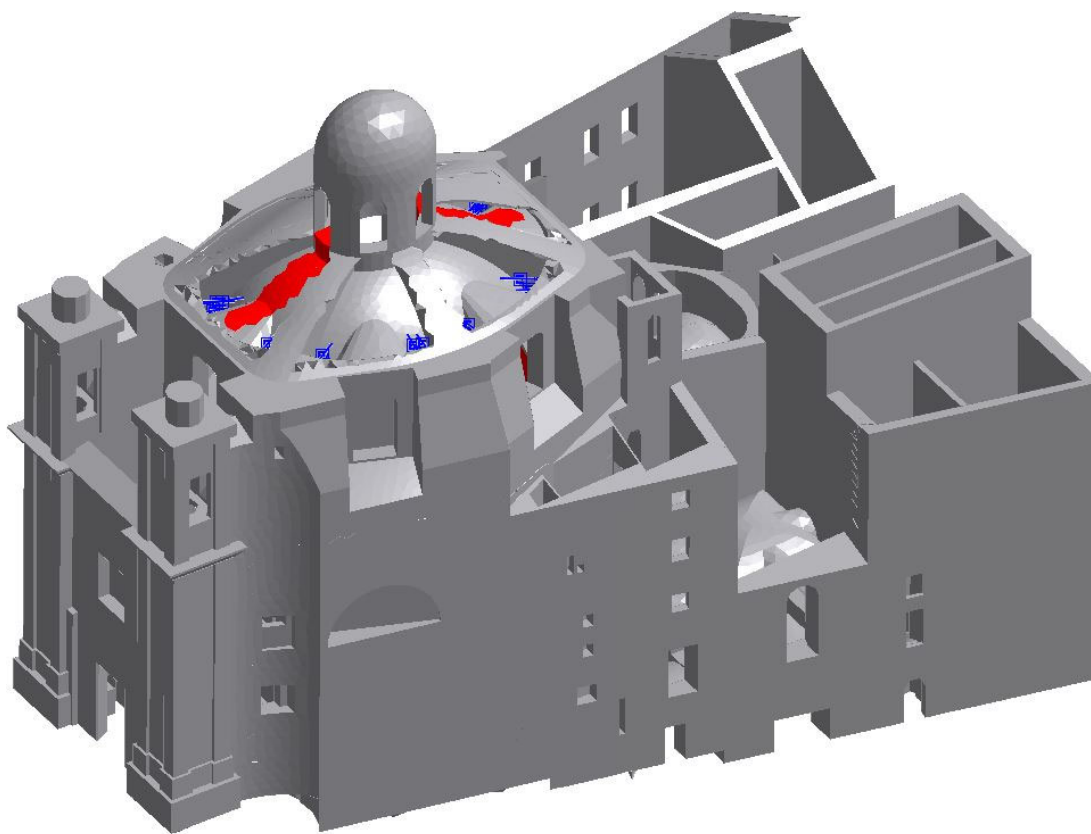


Figure 13. Section cut of the double shell ovoidal dome: the damaged masonry is shown in red and the compression-only spring elements are shown in blue.

The study aimed to focus on the structural behavior of the church; for this reason, the constraining effect of the annex Palazzo della Provincia was modeled by applying pinned condition to the boundary nodes of the east side.

The model was first analyzed in the elastic domain. In this initial phase, the material parameters (Young's modulus and mass density) and the stiffness of the point spring elements were defined with the information collected during the onsite testing campaign and then tuned up based on the global dynamic parameters resulting from the OMA through the semi-automated model updating method of Douglas-Reid [27]. This process, including a preliminary study on the most sensitive structural parameters, is described in detail in the following paragraphs.

4.1. Sensitivity Analysis

The global dynamic behavior is considered the reference experimental result for the model updating; thus, the numerical eigenvalues analysis of the FEM was used to select the most influential parameters for the dynamic behavior.

The relationship between the experimental dynamic behavior and the model parameters depends on the heterogeneity of the materials, including the possibility of unidentified damage (i.e., crack, loss of material/detachment, loose interlocking and microcracks), and the interaction among the structural elements, in particular, at the foundation level. In addition, the complexity of the model increases the number of parameters; for these reasons, the initially examined parameters were chosen based on engineering judgment and the already demonstrated influence of the boundary conditions [18,28].

First, the relevant parameters were estimated according to the results of the testing campaign and the gathered information on the construction stages of the church [8]: the

moduli of elasticity of the north and south exterior walls, the interior south masonry and the Palazzo della Provincia were obtained from the double flat jack tests; the interior North masonry was assumed with the same Young's modulus of the interior south side because it is the same type of structural element and the same period of construction. The dome and foundations moduli of elasticity were hypothesized as the average of the experimental moduli of the north and south exterior and interior masonry, while for the damaged masonry, which interests mainly the dome and part of the drum with the triumphal arch, it was considered a modulus of elasticity equivalent to one fifth of the dome. The modulus of elasticity of the façade was assumed as the average of the moduli of the north and south exterior masonries. The stiffness of the base springs was estimated through the Winkler's formulation considering a modulus of subsoil reaction equal to 36,000 kN/m³ as suggested by [29] for medium dense soils. As already considered in paragraph 3, a masonry density of 18 kN/m³ [15] was assumed and the sensitivity of the dome's masonry was analyzed separately (ρ_1) and the masonry of the rest of the church (ρ_2). The parameters are reported in Table 2.

Table 2. Model parameters influencing the dynamic behavior.

North exterior wall	E1	2800	MPa
South exterior wall	E2	4600	MPa
North internal masonry	E3N	1800	MPa
South internal masonry	E3S	1800	MPa
Dome	E4	2750	MPa
Damaged masonry	E5	550	MPa
Façade	E6	2750	MPa
Palazzo della Provincia	E7	1600	MPa
Foundations	E8	4833	MPa
Soil	K	6405	N/mm
Dome density	ρ_1	18	kN/m ³
Masonry density	ρ_2	18	kN/m ³

The evaluation of the relevant parameters was quantified with the sensitivity coefficient (2) according to [30], the sensitivity analysis considered an increment of 10% from the reference values of Table 2. In Equation (2):

$$S_{i,j} = 100 \cdot \frac{X_j}{R_i^{FEM}} \cdot \frac{\Delta R_i^{FEM}}{\Delta X_j} \quad \begin{matrix} i = 1, \dots, M \\ j = 1, \dots, N \end{matrix} \quad \begin{matrix} M = \text{Considered modes} \\ N = \text{Considered parameters} \end{matrix} \quad (2)$$

X_j represents the j^{th} model parameter;

R_i^{FEM} represents the i^{th} output of the analysis (the modal frequency);

ΔX_j represents the variation of the model parameter (10% increment from the initial value);

ΔR_i^{FEM} represents the variation of the output of the analysis.

The parameters with the highest sensitivity coefficient are those with major influence on the dynamic behavior. In Figure 14a, the average sensitivity coefficients are reported considering the first three modes of vibration with a total modal mass participation of 32.5, 46.7 and 65.5% respectively in X, Y and Z directions. The influence of the stiffness of masonry was also analyzed by comparing the volume (thus the number of finite elements) of each group respect the overall volume of the model as shown in Figure 14b.

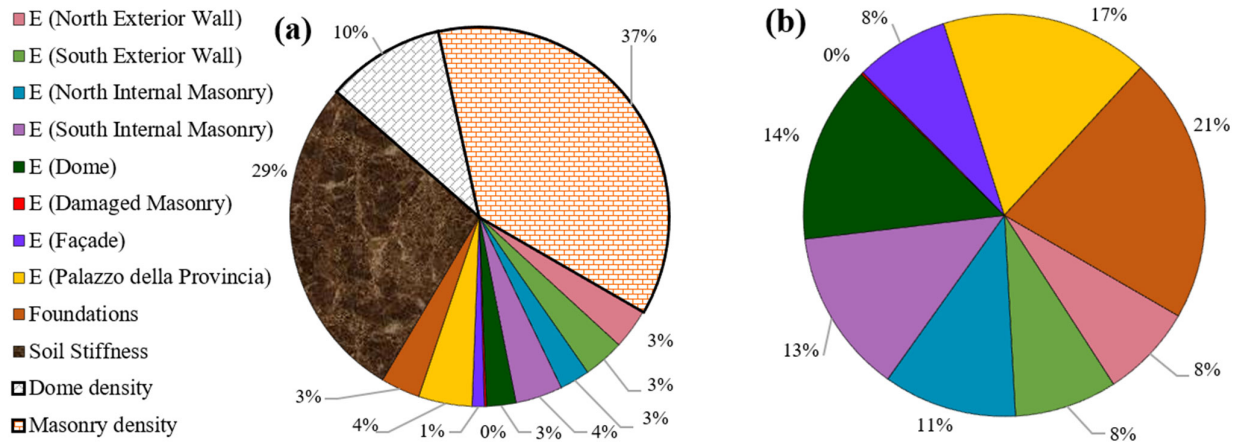


Figure 14. Average sensitivity coefficient: (a) considering the first three modes of vibration, (b) volumes of the groups respect the overall volume of the model.

The density of the material and the stiffness of the point springs resulted as the most influent parameters. The moduli of elasticity of the foundations, Palazzo della Provincia and façade returned modest sensitivity coefficients in comparison to their presence in the model; for this reason, they were discarded from the model updating. The damaged masonry represents a small part of the model with insignificant influence thus it was discarded as well from the model updating. The sensitivity analysis supported the selection of the relevant parameters for the model updating and it confirmed the major influence of the soil structure interaction in the dynamic behavior.

4.2. Semi-Automated Model Updating

The model updating is an iterative method, which aims at tuning up the physical parameters of a model until it reproduces the experimental data within a tolerated error.

The model updating procedure relies on the minimization of two quantities: the relative frequency error (Df_{ij}), defined in (3) and the modal assurance criterion (MAC_{ij}) [21], defined in (4).

$$Df_{ij} = \frac{f_{num,i} - f_{exp,j}}{f_{exp,j}} \cdot 100 \quad (3)$$

$f_{num,i}$ is the numerical frequency of the model and $f_{exp,i}$ the experimental frequency for the i^{th} mode of vibration.

$$MAC_{ij} \left(\left\{ \phi_{num,i} \right\}, \left\{ \phi_{exp,j} \right\} \right) = \frac{\left| \left\{ \phi_{num,i} \right\}^T \left\{ \phi_{exp,j} \right\} \right|^2}{\left(\left\{ \phi_{num,i} \right\}^T \left\{ \phi_{num,i} \right\} \right) \left(\left\{ \phi_{exp,j} \right\}^T \left\{ \phi_{exp,j} \right\} \right)} \quad (4)$$

$\phi_{num,i}$ is the numerical modal vector of the model and $\phi_{exp,i}$ is the experimental modal vector for the i^{th} mode of vibration.

In this work, the Douglas-Reid method was implemented to optimize the structural parameters of the FEM. The optimization is performed through an algorithm implemented in MATLAB [31] to minimize the objective function defined in (5) considering the first three modes of vibration ($M = 3$).

$$f(x) = \sum_{i=1}^M \left[(Df_{ii})^2 + \left(\frac{1 - \sqrt{MAC_{ii}}}{MAC_{ii}} \right) \right] \quad (5)$$

The experimental modal results obtained from the OMA were compared with the related output values obtained from the numerical eigenvalues analysis. The Douglas–Reid method uses an approximated model to interpolate with a quadratic function the structural parameters within a range of coordinate points representing the possible combination of parameters. The error reduction is performed by selecting the proper structural parameters from the set range of values using a batch analysis procedure.

The range of values was defined based on the reliability of the data and the variability of the typology of parameter. The moduli of elasticity of the north external wall, the south external wall and the south internal masonry estimated with the double flat jack tests and confirmed by the sonic tomography (southeast pillar) were set within a range of variation of $\pm 20\%$ since the results of the local tests are extended to a large volume of masonry, and it is reasonable to consider a scatter of the parameter from the reference experimental value. The moduli of elasticity estimated as the average of the experimental data (north internal masonry and dome) were set within a range of variation of $\pm 30\%$ due to the lack of information on the interested elements. A uniform density for both the church and its dome has been assumed, with a range of variation of $\pm 6\%$ because 1900 Kg/m^3 is considered the highest reasonable density for the brick masonry in question. On the other hand, the soil structure interaction was refined by dividing the spring supports in two independent groups (north and south) because of the different soil slope and further improved by disconnecting the stiffness of the point springs in the horizontal direction from the vertical direction. The four independent parameters representing the soil structure interaction were set within a range of variation of $\pm 20\%$.

The initial model parameters and their updated values are presented in Table 3.

Table 3. Model Updating parameters.

Model Parameter		Initial	Updated	Variation [%]
North Exterior Wall	E1 [MPa]	2800	3074	10
South Exterior Wall	E2 [Mpa]	4600	5520	20
North Internal Masonry	E3N [Mpa]	1800	1260	−30
South Internal Masonry	E3S [Mpa]	1800	1440	−20
Dome	E4 [Mpa]	2750	1925	−30
North Spring Vertical	Kz N [N/mm]	6405	7442	16
South Spring Vertical	Kz S [N/mm]	6405	5124	−20
North Spring Horizontal	Kxy N [N/mm]	641	769	20
South Spring Horizontal	Kxy S [N/mm]	641	769	20
Masonry Density	ρ [kN/m ³]	18	19.1	6

The model updating yielded to a reduction of the average frequency error of the first four modes of 2% (from 10.44% to 8.54%) as shown in Figure 15.

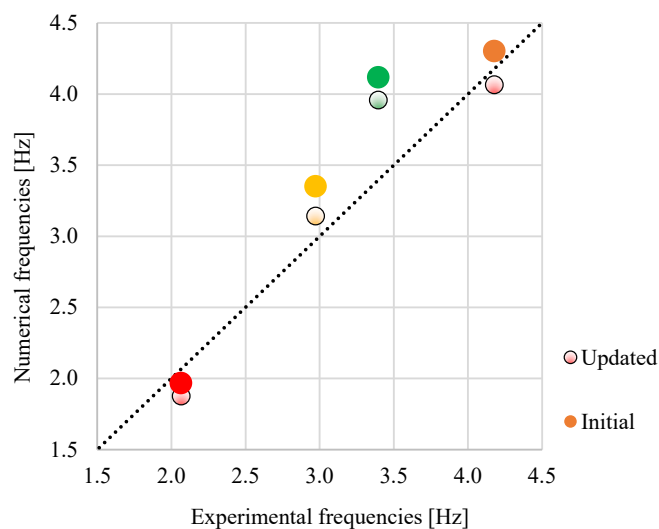


Figure 15. Frequency variation after model updating.

The modal deformations also returned an improvement, the gap between the numerical and the experimental modes decreased on average of 6.8% as reported in Figure 16 with the green columns. In addition, it was observed an increment of 6.6% of the independency for the different modes represented by the blue columns (although not included in the objective function) while the dependency between first-fourth and second-third modes resulted in an average divergence of 4.8% from the experimental modes as represented by the red columns.

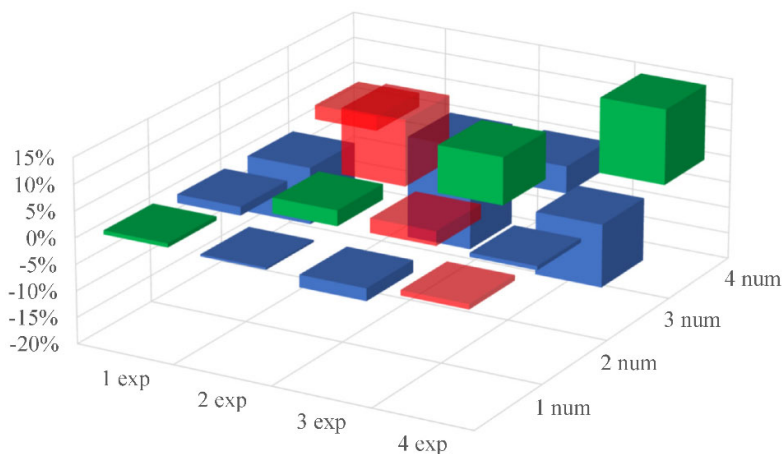


Figure 16. MAC variations between the numerical model due to the model updating: the improved modal displacements are shown in green and blue, and in red they are drifted apart from the experimental values.

The MAC of the updated model is reported in Figure 17 to highlight the affinity with the experimental MAC previously presented in Figure 11.

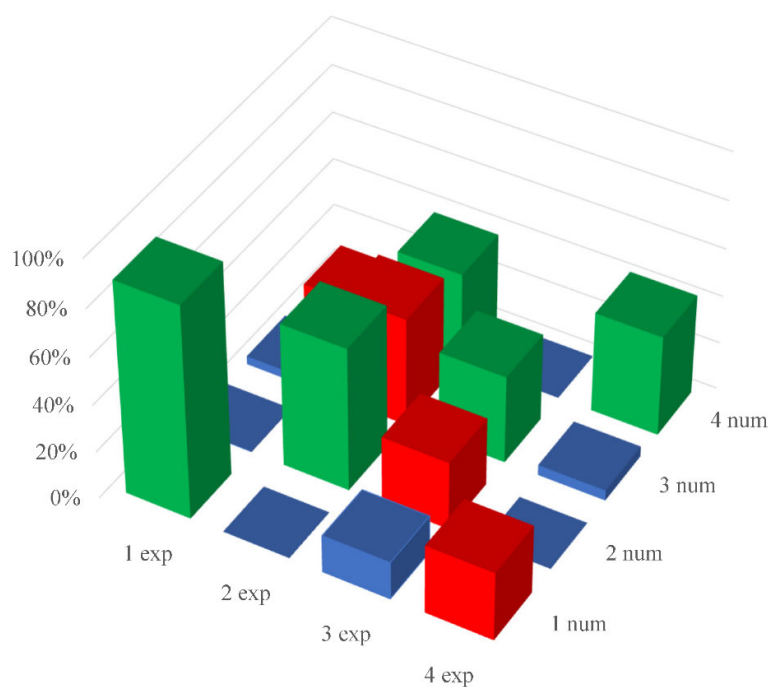


Figure 17. MAC between the experimental and the numerical modal shapes of the updated model: the improved modal shapes are in green and blue and, in red, they are drifted apart.

5. Nonlinear Analysis

Masonry being an heterogeneous material subject to important non linearities, it is essential to study the response of the structure in the nonlinear field. As presented in paragraph 4.2, the structural parameters of the model, which influence the linear response, were tuned up based on the on-site measurements, thus the updated model was further analyzed in the elasto-plastic domain by considering the damage plasticity constitutive model [32], which provides a general capability for the behavior of quasi-brittle materials under low confining pressures such as masonry.

5.1. Material Modeling

The used model describes the irreversible damage that occurs during the fracturing process considering the different reductions of the elastic stiffness when unloading for tension and compression and the stiffness recovery effects during cyclic load reversals. The model accounts for the damage variable, which assumes value equal to zero in absence of damage (elastic domain) and equal to one in case of total loss of strength.

The properties of the materials are considered differently according to the available experimental data. The Young's modulus, the mass density and the Poisson's ratios were already defined by the onsite testing and the model updating reported in Table 3 and Table 1. The nonlinear compressive behavior was described through the parabolic model given by Feenstra [33] in which both softening and limit strain depend on compressive fracture energy (G_c). Then, the material model was calibrated to match the envelop of the loading cycle resulting from the corresponding double flat jack test (DFJ) in Figure 18), the results from the test M3 have been applied to both the interior masonry on the south and north sides. The tensile behavior was described according to Hordijk [34] assuming tensile strengths equal to 6.7% of the corresponding compressive strength ($f_t = f_c/15$), the softening behavior is related to tensile fracture energy (G_t) through an equivalent crack length. The damage functions are derived from the stress-strain relationships of the materials. In

Figure 18, the constitutive laws of the tested materials used in the numerical model are represented.

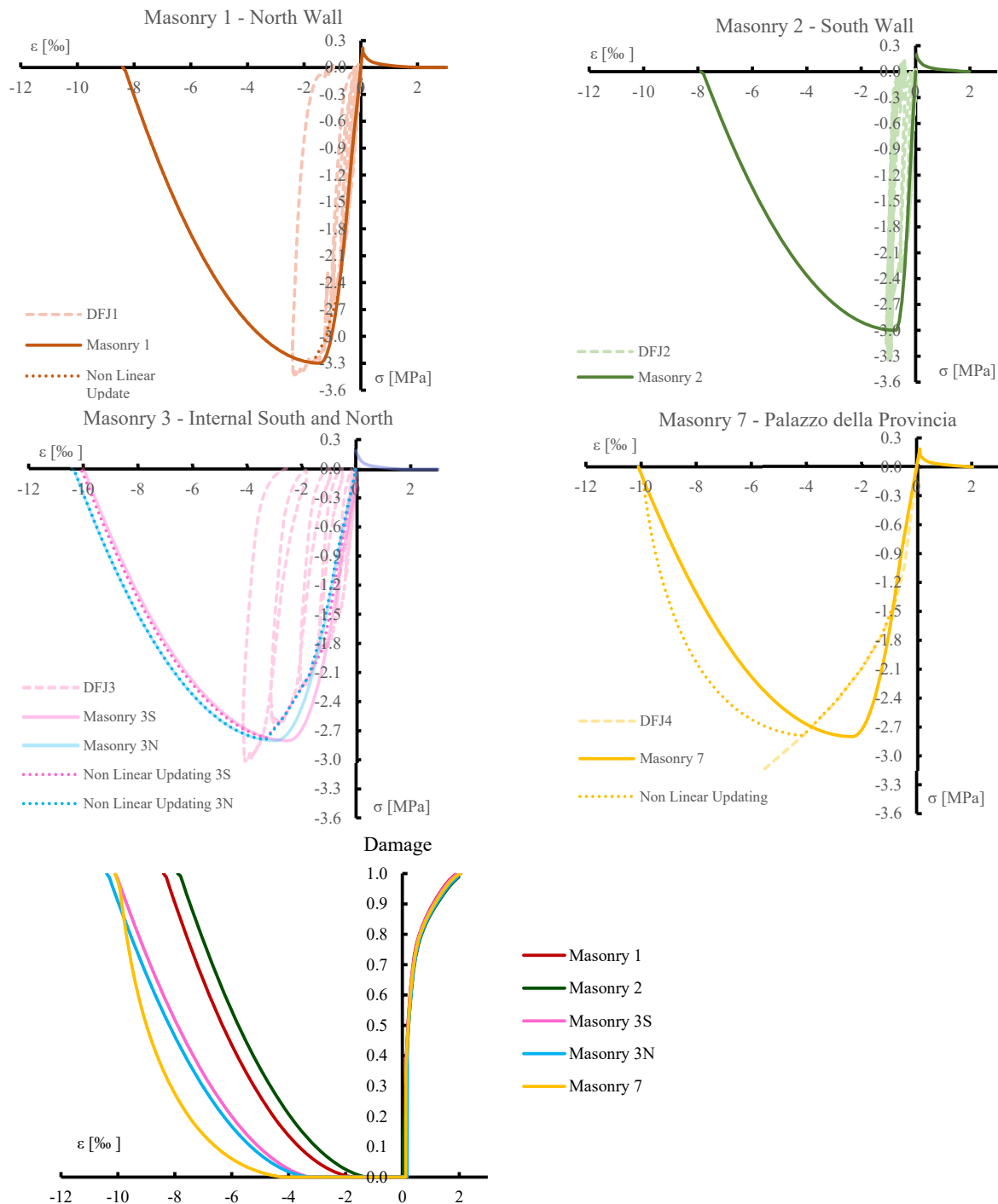


Figure 18. Stress–strain and damage–strain relationships for the materials with reference to the experimental data.

Regarding the materials without any specific on-site testing results, the stress–strain curves (Figure 19) were obtained from the average experimental values and considering the moduli of elasticity returned from the model updating, the compressive strength is assumed as the average compressive strength from all the double flat jack tests and the

other mechanical parameters (f_t , G_c , G_t , Damage) with the same criteria used for the tested materials.

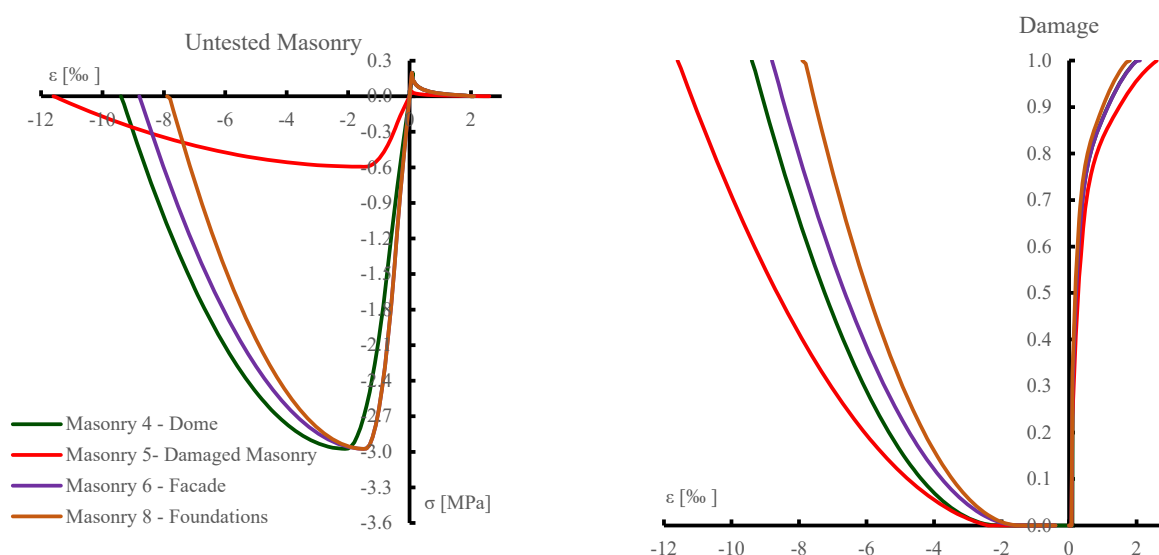


Figure 19. Stress–strain and damage–strain relationships for untested materials.

5.2. Nonlinear Static Analysis

The non-linear static analysis or pushover analysis simulates the response during an earthquake through the application of incremental horizontal forces until collapse. In this work, two distributions of lateral forces are applied to the model: uniform load pattern, in which the lateral forces are proportional to the mass, and modal pattern, in which the lateral forces are proportional to the main mode shapes (from the numerical modal analysis: the first mode with 45% of modal effective mass in the y-direction and the second mode with 22% of modal effective mass in the x-direction). Thus, a total of eight pushover analyses were performed according to the previously mentioned load distributions and the positive and negative principal directions. The convergence criterion is based on the energy control with a tolerance of 0.01 from the i^{th} to the $i^{\text{th}}+1$ iteration step. The response of the structure is represented by the capacity curve, which reports the value of the seismic coefficient (6) versus the displacement of a control point.

$$\alpha_i = \frac{\sum_i \text{Horizontal Force}}{\text{Self Weight}} \quad (6)$$

where i is either the horizontal direction x or y .

The MDOF system of the church is transformed to a SDOF by dividing the seismic coefficient and the nodal displacement by the modal participation factor Γ .

In Figure 20a, the capacity curves are compared with the seismic demand represented by the acceleration–displacement response spectrum (ADRS), the analysis in the longitudinal X direction return capacity curves for both load patterns with higher capacity of the structure in the positive direction (east side) are constrained by Palazzo della Provincia, while the negative X direction highlights the high risk of the façade to overturn out of plane.

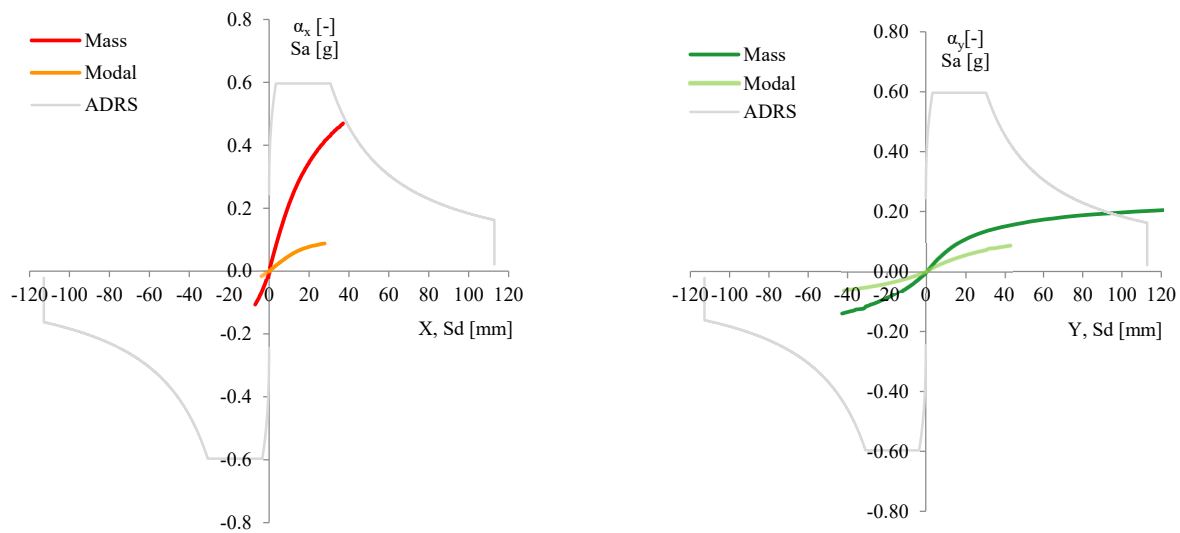


Figure 20. Capacity curves from nonlinear static analysis, (a) in the X direction, (b) in the Y direction.

In Figure 20b, the analysis in the longitudinal Y direction returns capacity curves of both the load patterns with higher capacity of the structure in the positive Y direction (north side, uphill). Although, the geometry of the church is essentially symmetric, the higher ground level of the north side together with the mechanical characteristic of the north exterior masonry (lower stiffness but larger resistance than the south side) contributes to the larger seismic coefficient and admissible deformation of the church in the positive Y direction.

5.3. Nonlinear Dynamic Analysis

Nonlinear time-history analysis was performed using the three synthetic accelerograms generated from the elastic design spectra according to the Italian Code [15] at the ultimate limit State (SLV) with the software SIMQKE [35] reported in Figure 21, where SLV EQX, EQY and EQZ are the spectra of the accelerograms in the three principal directions. The accelerograms were applied in the three directions, for a total duration of 10 seconds due to the cumbersome of the computer runs.

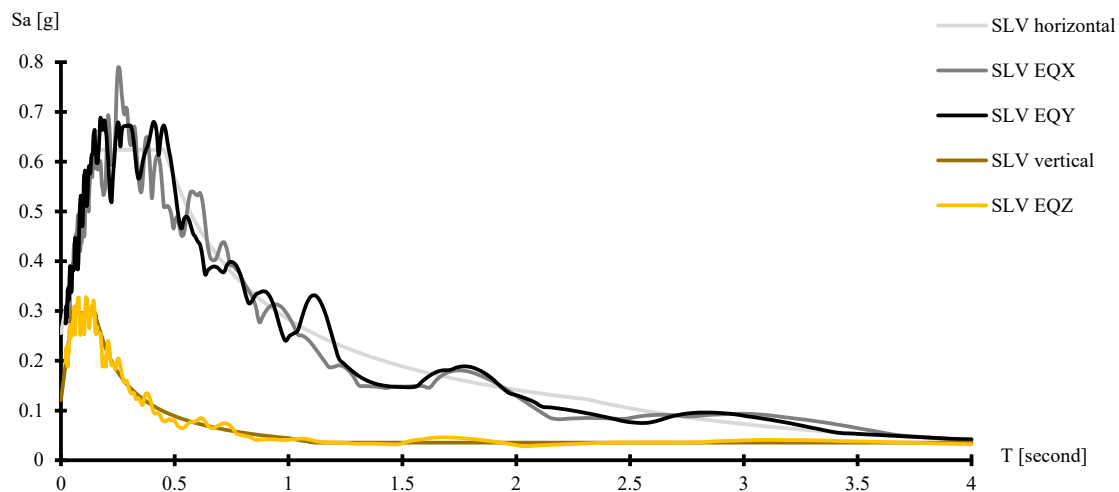
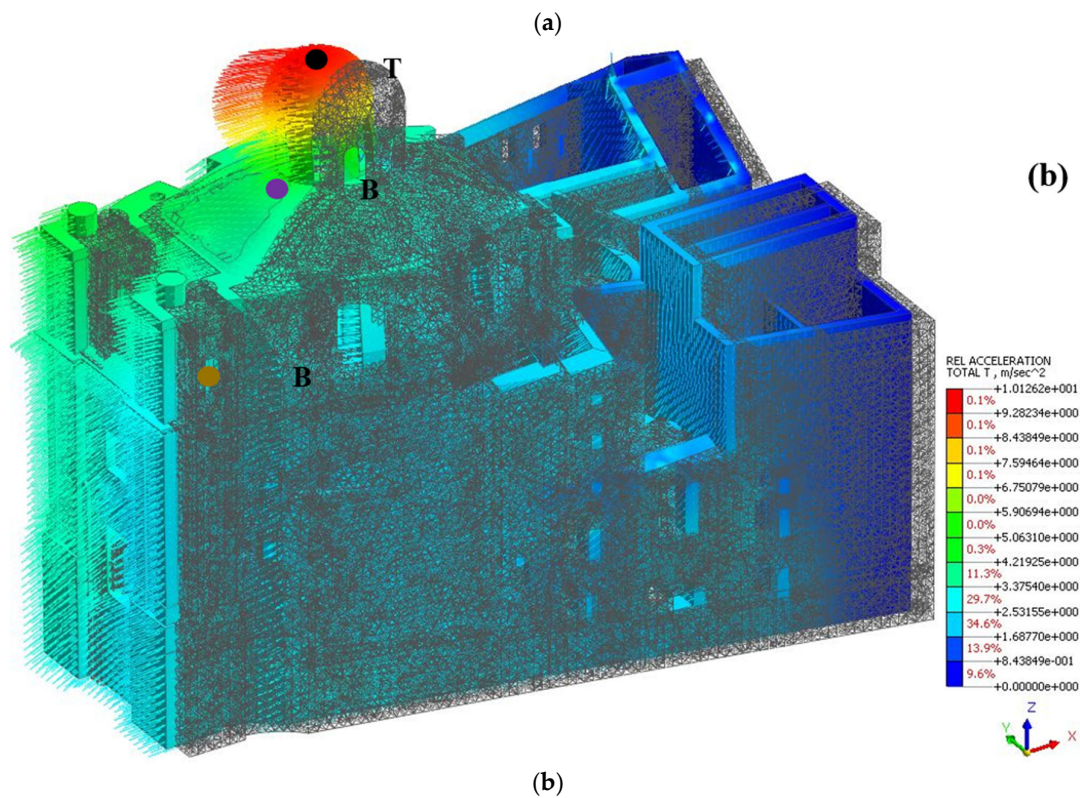
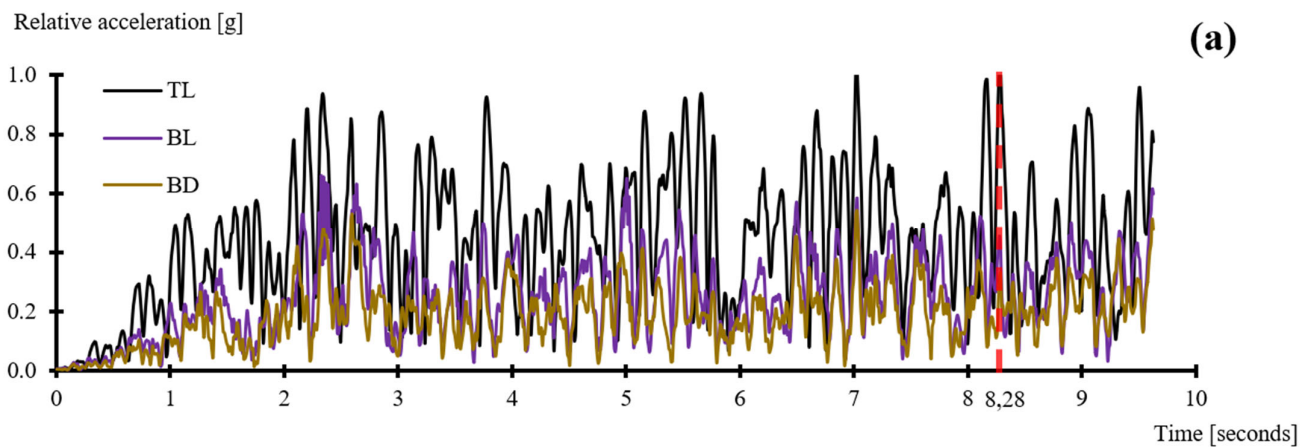


Figure 21. Horizontal and vertical elastic response spectra in Macerata with synthetic generated accelerograms.

First, the three control points are defined based on the expected maximum drifts: TL (top of the lantern), BL (base of the lantern) and BD (base of the dome). The moduli of the relative acceleration are monitored over the time history analysis as reported in Figure 22a. The maximum acceleration results at 8.28 seconds in node TL positioned at 35.6 m height. At this time step, the displacements of the three control points are linearly proportional to the height of the structure, thus no relevant damage appears yet, as shown in Figure 22b. However, the acceleration of node TL results 3.4 times higher than BD and the acceleration of BL results 1.5 times higher than BD. This means that the lantern is subject to higher accelerations than the rest of the structure because of the dynamic amplification, this effect yields to the formation of local collapse mechanism with the persisting of the earthquake.



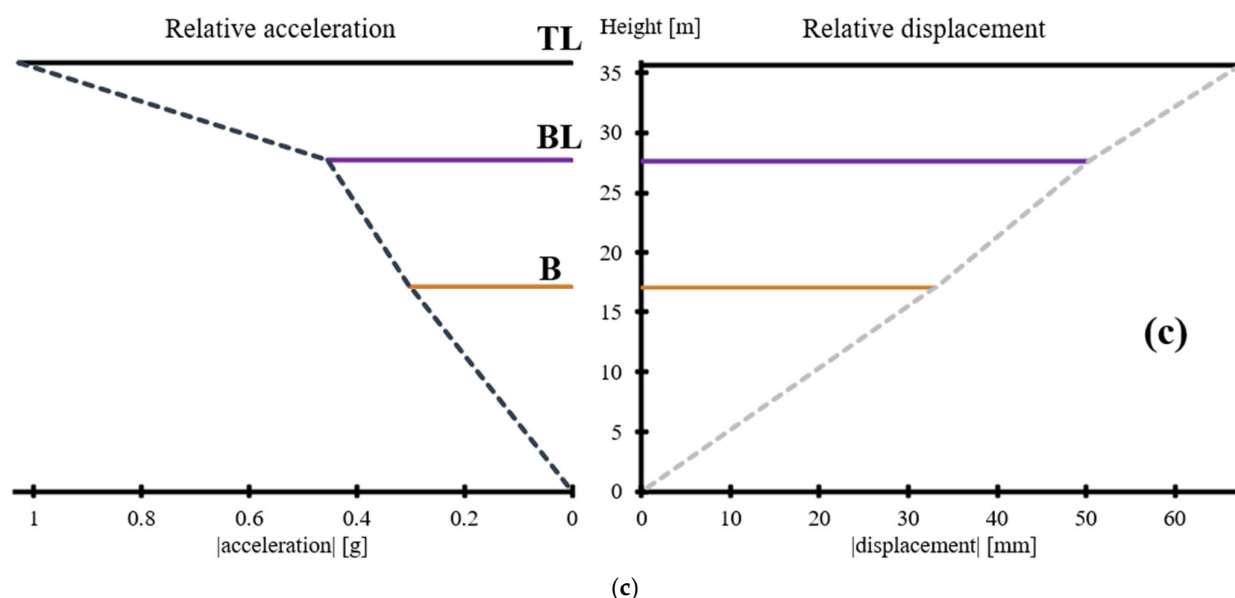


Figure 22. (a) Time history acceleration of the control points, (b) deformed shape and relative total acceleration at 8.28 s and (c) relative total acceleration and total displacement of the control points along the height of the structure.

The structural response of the model is analyzed in Figure 23, considering the longitudinal direction (X) by comparing the displacement of the control point TL with the seismic coefficient (α_s) and the corresponding maximum principal strain distribution (tensile deformation). The time history highlights the residual translation of control point TL towards the negative X direction (façade side), the principal strain status during the maximum positive displacement (6.4 mm) in Figure 23a shows reasonable homogeneous distribution due to the small seismic excitation. Starting from the maximum seismic coefficient (0.24) in Figure 23b, the critical portions of masonry are identified in correspondence of the central part of the façade and the dome along the longitudinal direction. At the maximum seismic coefficient in the negative direction (−0.23) shown in Figure 23c, the principal strains increase by one or two orders of magnitude and all the potential collapse mechanisms emerge (roof of Palazzo della Provincia, central portion of the south wall, roof of the sacristy on the southeast side, south-west diagonal crack of the dome) which are confirmed by the last plot during the maximum negative displacement (−54 mm) shown in Figure 23d, corresponding to the maximum concentrations of principal strains as a response to the maximum seismic coefficient in the negative direction and the accumulated damage.

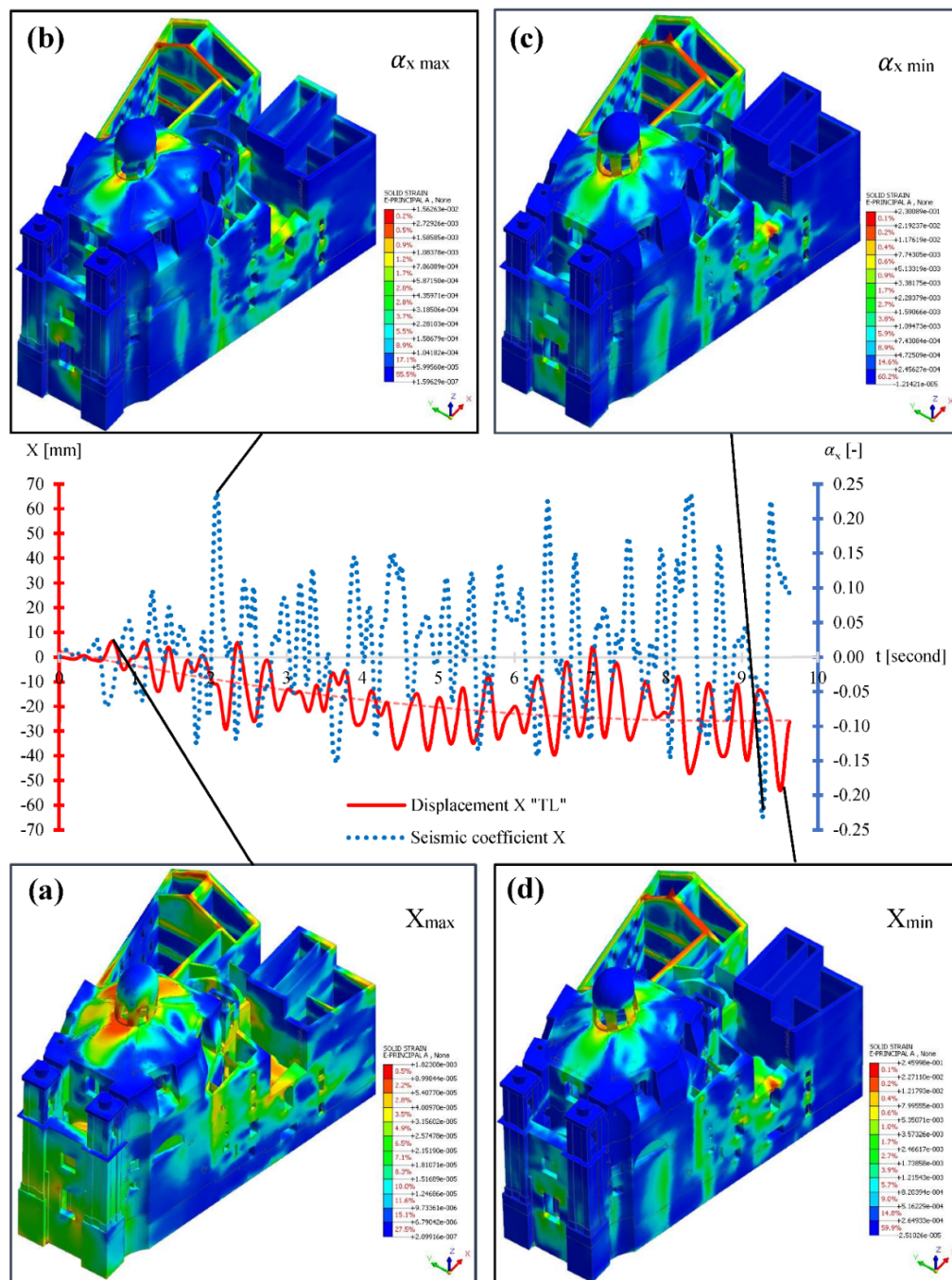


Figure 23. Structural response for the NLTH in the longitudinal X-direction: (a) maximum positive displacement in X, (b) maximum positive seismic coefficient X, (c) maximum positive displacement in X and (d) maximum positive displacement in X.

The nonlinear dynamic response is also analyzed considering the transversal direction (Y) in Figure 24. Along the transversal direction, control point TL performs large oscillations around the initial position highlighting higher deformation capacity than the longitudinal direction without any evident residual displacements. The distribution of maximum tensile principal strain during the maximum seismic coefficient in the negative direction (-0.16) and the consequent maximum displacement (63 mm) in Figure 24a,b shows the presence of the already mentioned potential collapse mechanisms, in addition to the warning due to stress and strain concentration at the base of the two façade towers.

The principal tensile strains with the maximum seismic coefficient in the positive direction (0.20) and the maximum translation in the negative direction (−36 mm) shown in Figure 24c,d report similar distribution and magnitude although spaced by a time lapse of 2.5 seconds. In the second half of the earthquake, the structure developed the necessary deformations and its movements settled.

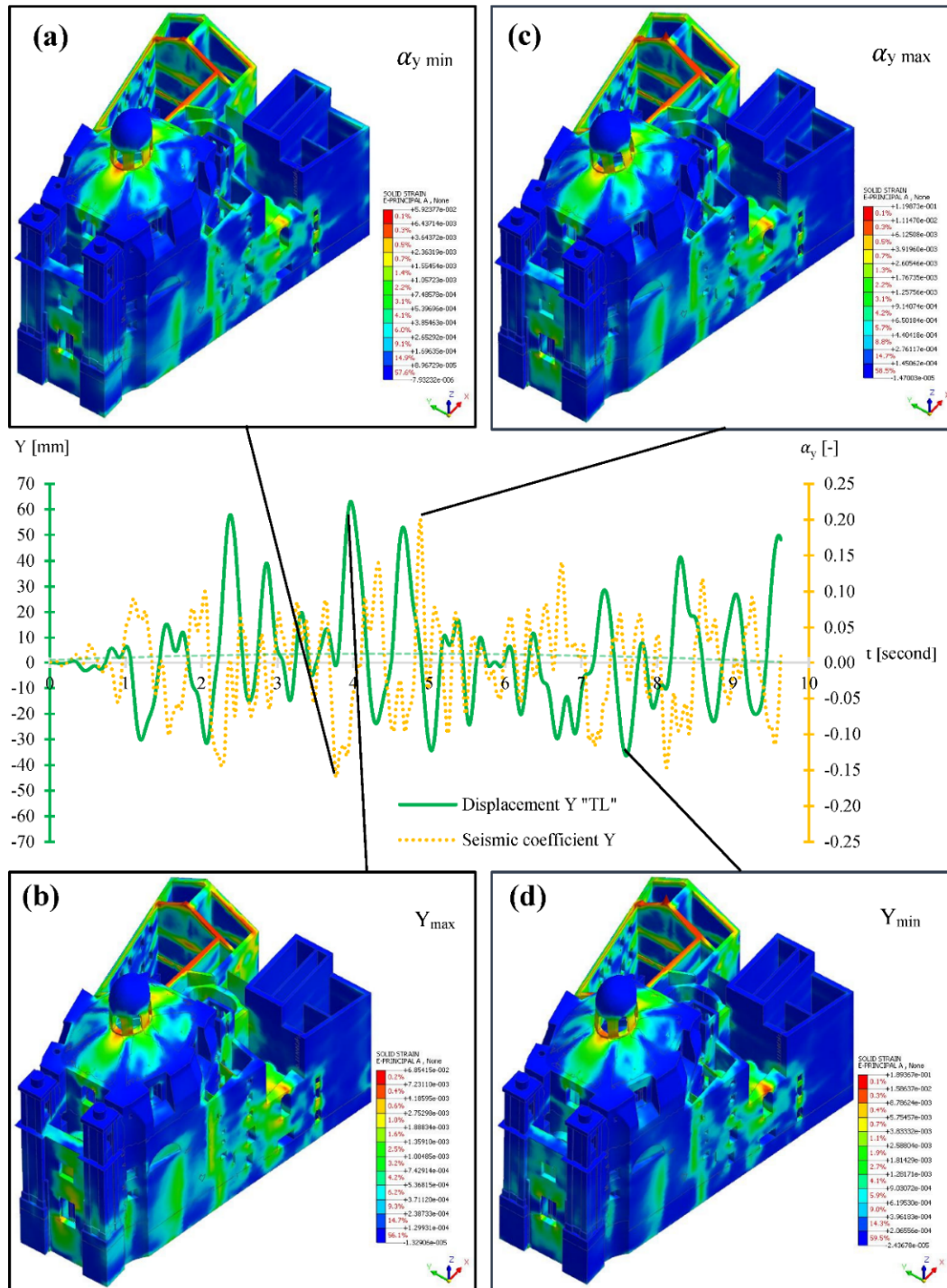


Figure 24. Structural response for the NLTH in the transversal Y-direction: (a) maximum positive displacement in Y, (b) maximum positive seismic coefficient X, (c) maximum positive displacement in X and (d) maximum positive displacement in X.

By comparing the overall principal strains and displacements, of interest is the relevance of the first seconds of the earthquake on the structural response where the main damage is likely concentrated, confirmed by the development of the residual X translation in the negative direction of Figure 23, which tends to settle.

In Figure 25 shows the horizontal trajectory of the control point TL during the nonlinear time history analysis. The point follows a chaotic path shifted in the negative X (west side) and slightly shifted towards the positive Y (north side) as also reported in the nonlinear static analysis results presented in Section 5.2 (Figure 20).

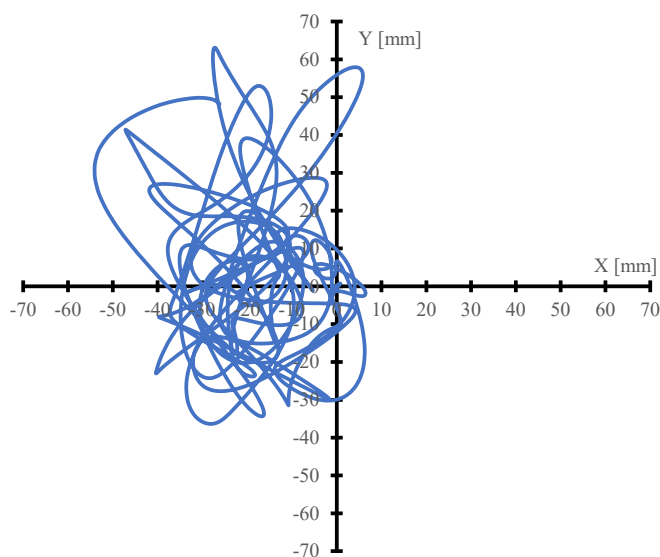


Figure 25. Horizontal trajectory of the control point TL during the nonlinear dynamic analysis.

The evolution of the seismic coefficient vs the displacement along the two principal directions is plotted in Figure 26. In Figure 26a along the X direction, larger displacements in the negative direction (west side) are caused by the tendency of the church to deform toward the façade, while in the positive direction (east side); the structure is constrained by the Palazzo della Provincia. In Figure 26b, the curve shows larger displacements in the positive Y direction (north side); this effect is caused by the different stiffness of the two sides of the church. The envelopes of the displacements confirm the lower stiffness of the structure and the larger dissipation capacity in the transversal Y direction, which is also connected by the presence of the modeled longitudinal crack that facilitates the energy dissipation. The comparison of the seismic demand and the resulting displacements shows almost the same safety margins with a slightly higher margin of safety in the transversal direction.

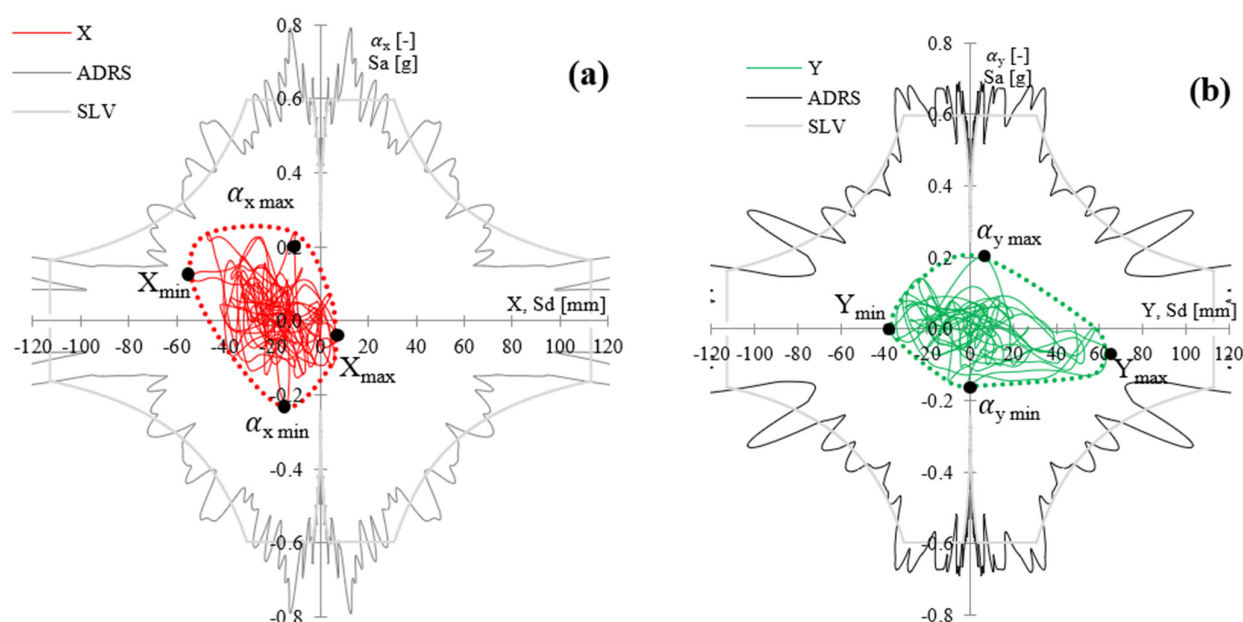


Figure 26. Nonlinear dynamic analysis: seismic coefficient evolution respects the displacement of the control point TL, in (a) considering the longitudinal X-direction, in (b) considering the transversal Y-direction.

5.4. Results and Discussion

The displacement response obtained by the non-linear static analysis is in reasonable agreement with the response from the nonlinear dynamic analyses. The nonlinear dynamic analysis provides displacement capacity lower than the results from the pushover analysis considering the mass proportional load, while the modal pushover analysis returned the most conservative results out of all the performed analysis. In historical masonry buildings, the complex architectural forms and the existing damage play a relevant role in the seismic response of the structure. The nonlinear dynamic analysis accounts for the effects of the inertia and a wider number of modes, including possible higher local modes; however, the results are complex to interpret due to the random nature of the excitation.

The nonlinear static analysis returns an overall simplified representation of the expected deformation under lateral loads, the mass proportional load uniformly encompassed the entire church while the modal proportional load focused on the top lantern highlighted the vulnerability of the base of this element. The choice of the control point is a critical issue since the resulting capacity significantly depends on the location of it. On the other hand, pushover analysis is more manageable and requires a lower computational burden. As a consequence, it is well codified in standards [15,36,37] and often applied in research and professional work.

6. Conclusions

A comprehensive study on the nonlinear seismic response of an historical masonry church was performed through a complex finite element model based on experimental measures. The results from the onsite testing (double flat jack test, video endoscopy and sonic tomography) and monitoring campaign (ambient vibration test) on the church of San Filippo Neri in Macerata were reported and implemented in an advanced numerical model. The ambient vibration test and the operational modal analyses successfully returned accurate information on the modal parameters of the church (natural frequency, modal shape vectors and modal damping of the first four modes of vibration), the result was used to refine the information on the different stiffnesses of the masonry by

subdividing the model in several groups of elements, and to estimate the relevant influence of the soil–structure interaction through the semi-automated Douglas-Reid model updating method. The modal behavior of the updated numerical model is sufficiently close to the experimental values; it was not possible to further reduce the error by varying the most sensitive parameters. Additional effort is required to model other characteristics of the building (discontinuity due to the longitudinal crack, refinement on the mass distribution and flexible lateral constraints to model the influence of the lateral building).

Static and dynamic nonlinear analyses were performed and compared to study the seismic behavior of the church. Both the analysis returned qualitative results in terms of capacity in agreement with the expected behavior and the complexity of the church. The quantitative outcome is sensitive to the dynamic behavior and choice of the control points. Once the qualitative behavior is established, the comparison of multiple control points becomes a fundamental aspect to take into consideration in the quantitative evaluation of the seismic capacity. The performed analyses prove the capability of the methodology that integrates onsite testing, ambient vibration testing with the sensitivity analysis and the model updating to tune up an advanced finite element model. The numerical simulation supported the intuitive detection of the critical locations, and it highlighted the relevance of local failure mechanisms over the global response of the systems. The methodology allows for the design of a minimal strengthening intervention to achieve a high level of safety compatible with both the need of protection and conservation of historical monuments. Refined numerical models updated by means of onsite experimental testing together with nonlinear analysis are capable to evaluate the present structural conditions, predict the behavior under severe events and propose an accurate strengthening intervention for which other simplified models and analysis are not able to perform. The great efforts of this methodology are challenging the community that struggles to adopt onsite testing and dynamic identification in the model definition, as well as nonlinear analysis in the structural verifications of masonry constructions. Simpler tools and methods are commonly used in professional practice; the effort is indeed less at the expense of the accuracy and thus requires minimal intervention. This work intends to disseminate proper conservation practices for historical masonry constructions and facilitate the interpretation of the results of nonlinear analysis.

Author Contributions: Supervision S.S. and C.B.; methodology, S.S. and V.S.; formal analysis, V.S. and C.S.; investigation, V.S. and C.S.; writing—original draft preparation, S.S. and V.S.; writing—review and editing, S.S. and V.S. All authors have read and agreed to the published version of the manuscript.

Funding: This research received no external funding

Acknowledgments: The authors are grateful to the Diocesi of Macerata and Da Gai Studio for the geometrical survey and the technical reports. They also thank Lorena Sguerri and Giovanni Barco from PRiSMa Laboratory of Roma Tre University for the cooperation during the testing campaigns.

Conflicts of Interest: The authors declare no conflict of interest.

References

1. Neal, C. "Truth Unveiled: Bernini's Bell Towers and the Allegory of Truth: The Bell Tower Disaster," *Gianlorenzo Bernini: An Online Exhibit by Students in ARTH 470s: Bernini, in the Department of Art and Art History, University of Mary Washington*; Springer: Berlin/Heidelberg, Germany, 2013. <https://bernini2013.org/truth-unveiled-by-time/the-bell-tower-fiasco/>. (September 2021).
2. Baggio, C. Il restauro antisismico dei centri storici e la regola d'arte. *Ricerche di Storia dell'arte, Volume 3*, **2009**, 32, 19–30. doi: 10.7374/71462
3. Roca, P.; Cervera, M.; Gariup, G. Structural analysis of masonry historical constructions. Classical and advanced approaches. *Arch. Comput. Methods Eng.* **2010**, 17, 299–325.
4. Mendes, N.; Lourenço, P.B. Seismic Assessment of Masonry "Gaioleiro" Buildings in Lisbon, Portugal. *J. Earthq. Eng.* **2009**, 14, 80–101, doi: 10.1080/13632460902977474.
5. D'Ambrisi, A.; Mariani, V.; Mezzi, M. Seismic assessment of a historical masonry tower with nonlinear static and dynamic analyses tuned on ambient vibration tests. *Eng. Struct.* **2012**, 36, 210–219.

6. Valente, M.; Milani, G. Non-linear dynamic and static analyses on eight historical masonry towers in the North-East of Italy. *Eng. Struct.* **2016**, *114*, 241–270.
7. Ricci, A. *Memorie Storiche Delle Arti e Degli Artisti Della Marca di Ancona*; Tipografia di Alessandro Mancini, Con Approv., Macerata, Italy, 1834; Volume 1.
8. Chiesa di San Filippo Neri a Macerata. Available online: <http://www.sanfilippomc.it/la-storia> (10 June 2021).
9. A. Rovida, M. Locati, R. Camassi, B. Lolli, P. Gasperini, and A. Antonucci, “The Italian Earthquake Catalogue CPTI15—Version 3.0,” Ist. Naz. Geofis. E Vulcanol. INGV, Rome, Italy, 2021.
10. S. Pondrelli, European-Mediterranean Regional Centroid-Moment Tensors Catalog (RCMT) [Data set], Istituto Nazionale di Geofisica e Vulcanologia (INGV). 2002. <https://doi.org/10.13127/rcmt/euromed> (01 December 2021)
11. Terremoto: Inagibile il duomo di Macerata, Cronache Maceratesi, 2016. Available online: <https://www.cronachemaceratesi.it/2016/08/25/terremoto-inagibile-il-duomo-di-macerata/850291/> (10 January 2021).
12. ASTM. C1197-09: Standard Test Method for In Situ Measurement of Masonry Deformability Properties Using Flat-Jack Method. West Conshohocken, PA, USA, 2009, doi: 10.1520/C1197-09 (10 January 2021).
13. E. UNI. 1052-1 (2001), *Methods of tests for masonry: Determination of Compressive Strength*, 2001 (10 January 2021).
14. Adding and Solgeo, *aTom Software*. 2020.
15. Ministero delle Infrastrutture e dei Trasporti, *Istruzioni per l'applicazione dell'«Aggiornamento delle “Norme tecniche per le costruzioni”» di cui al decreto ministeriale 17 gennaio 2018.*, Rome, Italy, 2019.
16. Mehta, P.K.; Monteiro, P.J.M. *Concrete-Microstructure, Properties, and Materials*, McGraw-Hill Education, 3rd ed. New York, 1993.
17. Lydon, F.D.; Balendran, R.V. Some observations on elastic properties of plain concrete. *Cem. Concr. Resear.* **1986**, *16*, 314–324.
18. Baggio, C.; Sabbatini, V.; Santini, S. Model updating of a masonry historical church based on Operational Modal Analysis: The case study of San Filippo Neri in Macerata, In Proceedings of the COMPDYN 2019: 7th International Conference on Computational Methods in Structural Dynamics and Earthquake Engineering, Crete, Greece, 24–26 June 2019; Papadrakakis, M., Fragiadakis, M., Eds.; Volume 2, pp. 3777–3792.
19. Peeters, B.; Van der Auweraer, H.; Guillaume, P.; Leuridan, J., The PolyMAX Frequency-Domain Method: A New Standard for Modal Parameter Estimation?. *Shock and Vibration*; 2004; Volume 11, 395–409.
20. V, S.I.S.N. *Simcenter Testlab Software*; Siemens, 2018.
21. Allemang, R.J.; Brown, D.L. A correlation coefficient for modal vector analysis. In *1st International Modal Analysis Conference*; Orlando, Florida, USA, 1982; Volume 1, pp. 110–116.
22. *Midas Fea NX*. MIDAS Information Technology Co., 2015.
23. Elyamani, A.A.M. *Integrated Monitoring and Structural Analysis Strategies for the Study of Large Historical Construction. Application to Mallorca Cathedral*; Universitat Politècnica de Catalunya: Barcelona, Spain, 2015.
24. Serlio, S. *The Five Books of Architecture*; Dover Publications, 1982.
25. Conforti, C.; Editore, A.M. *Lo Specchio del Cielo: Forme Significati Tecniche e Funzioni Della Cupola dal Pantheon al Novecento*; Electa Milan, Italy, 1997.
26. Becchi, A.; Foce, F. *Degli Archi e Delle Volte: Arte del Costruire tra Meccanica e Stereotomia*; 2002.
27. Douglas, B.M.; Reid, W.H. Dynamic tests and system identification of bridges. *J. Struct. Div.* **1982**, *108*, 2295–2312.
28. Baggio, C.; Sabbatini, V.; Santini, S.; Sebastiani, C. Comparison of different finite element model updates based on experimental onsite testing: the case study of San Giovanni in Macerata. *J. Civ. Struct. Health Monit.* **2021**, *11*, 767–790.
29. Bowles, J.E. *Foundation Analysis and Design*, 5th ed.; McGraw-Hill: New York, USA, 1996.
30. Mottershead, J.E.; Link, M.; Friswell, M.I. “The sensitivity method in finite element model updating: A tutorial. *Mech. Syst. Signal Process.* **2011**, *25*, 7, doi: 10.1016/j.ymssp.2010.10.012.
31. Simulink, *MATLAB R2019a*; 2019.
32. Jeeho, L.; Fenves Gregory, L. Plastic-Damage Model for Cyclic Loading of Concrete Structures. *Journal of Engineering Mechanics*. **1998**, Volume 124, issue 8, 892–900, [https://doi.org/10.1061/\(ASCE\)0733-9399\(1998\)124:8\(892\)](https://doi.org/10.1061/(ASCE)0733-9399(1998)124:8(892)).
33. Feenstra, P.H. Computational Aspects of Biaxial Stress in Plain and Reinforced Concrete. Ph.D. Thesis, Delft University of Technology, Delft, Netherlands, 1993.
34. Hordijk, D.A. Local Approach to Fatigue of Concrete. Ph.D. Thesis, Delft University of Technology, Delft, Netherlands, 1991.
35. Gelfi. *SIMulation of earthQuAKE Ground Motions*;
36. ASCE. *Seismic Evaluation and Retrofit of Existing Buildings*; American Society of Civil Engineers: 2017.
37. Kariotis, J.C. *Methodology for Mitigation of Seismic Hazards in Existing Unreinforced Masonry Buildings: Categorization of Buildings*; ABK-A Joint Venture: 1981.